

Supplemental Information for “Size-dependent kinetic restructuring of catalyst active sites: A MACE-APE study of fluxional Pdn/MgO (n=3-11) clusters”

Patricia Poths,^{*a} King Chun Lai^b Christoph Scheurer^a, Sebastian Matera^a, and Karsten Reuter^a

Supplemental Note 1: MACE training set, parameters, and accuracy

The MACE framework is an extension to the Atomic Cluster Expansion (ACE), which incorporates message-passing neural networks in the calculation of the local atomic environments. For the MACE potential constructed for this work, we use 2 message-passing layers, each with 64 channels, and equivariant messages of the order $L=1$. Batch sizes of 16 structures were used for the training and validation sets. The potential was optimized over 250 epochs. Energy and force data was weighed equally at 1000 each. An exponential moving average (EMA) was used throughout the training process, with stochastic weight averaging (SWA) from epoch 150 onwards. The Mean absolute error (MAE) was used as the evaluation metric for the training, assessed on a validation set consisting of a fraction of 0.05 of the final training set.

The accuracy of the final MACE potential used in this work is shown in the table below.

	MAE E / meV/atom	MAE F / meV/Å	Relative F MAE %
Training set	3.4	12.6	10.30
Validation set	7.5	15.6	11.45

The training set consisted of 2404 structures, 3 of which were the isolated atom energies, which serve as the reference for the atomic energies of the condensed phase. The remaining 2401 structures also contain 130 atom pairs, 146 Pd and MgO bulk and surface structures, with the remaining structures consisting of 1-23 Pd atoms on a fixed MgO support containing 256 Mg and O atoms. For the APE-derived structures, which consisted of 49% (1047 structures) of the remainder of the training set (2,125 structure), there were slightly more TS structures than LM structures. This was not enforced, but arose naturally from the DECAF selection of new structures from APE with new local atomic environments not represented in the previous training set. Non-APE-derived structures, which consisted of the initial training set required to enable APE exploration with a preliminary MACE potential were derived from MACE MP0-MD and dimer search structures.

The accuracy of the barriers is shown in the table below, in terms of the root mean squared error and standard deviation of the DFT barriers and reaction energies compared to the MACE values, calculated for 1268 barriers extracted from APE outputs. 10% of the unique APE-obtained barriers for each cluster size were chosen for validation.

	rmse (eV)	std (eV)
Barrier height	0.073	0.063
Reaction energy	0.080	0.079

Note that these errors are less than the typical error expected from DFT, which is ~ 0.2 eV. Thus, we can assume that the MACE potential is a suitable surrogate model for the DFT PES.

Supplemental Note 2: APE parameters

The APE parameters for this work required a minor update relative to our previous work on O-induced restructuring of a Pd step-edge. The parameters which were suitable for exploring surface restructuring were too harsh for exploring the dynamics of cluster restructuring, leading to a higher proportion of “not connected” failures of the dimer search. Rather than SOAP for the DECAF classification of local atomic environments, we used the MACE model associated with the potential. The parameters that we updated relative to the previous work are:

Parameter	Value	Note
displace_max_coordination	7	
displace_radius	2.75	
displace_magnitude	0.175	
max_single_displace	2.75	
max_step_size	0.20	Slightly decreased
nonlocal_count_abort	6	Number at which moving more than this number of atoms terminates the dimer search
opt_method	cg	Previous algo FIRE resulted in too many “Not-connected” termination of dimer searches; conjugate gradient resulted in much better success rates

For the submit file for APE, please see the .zip file associated with the SI.

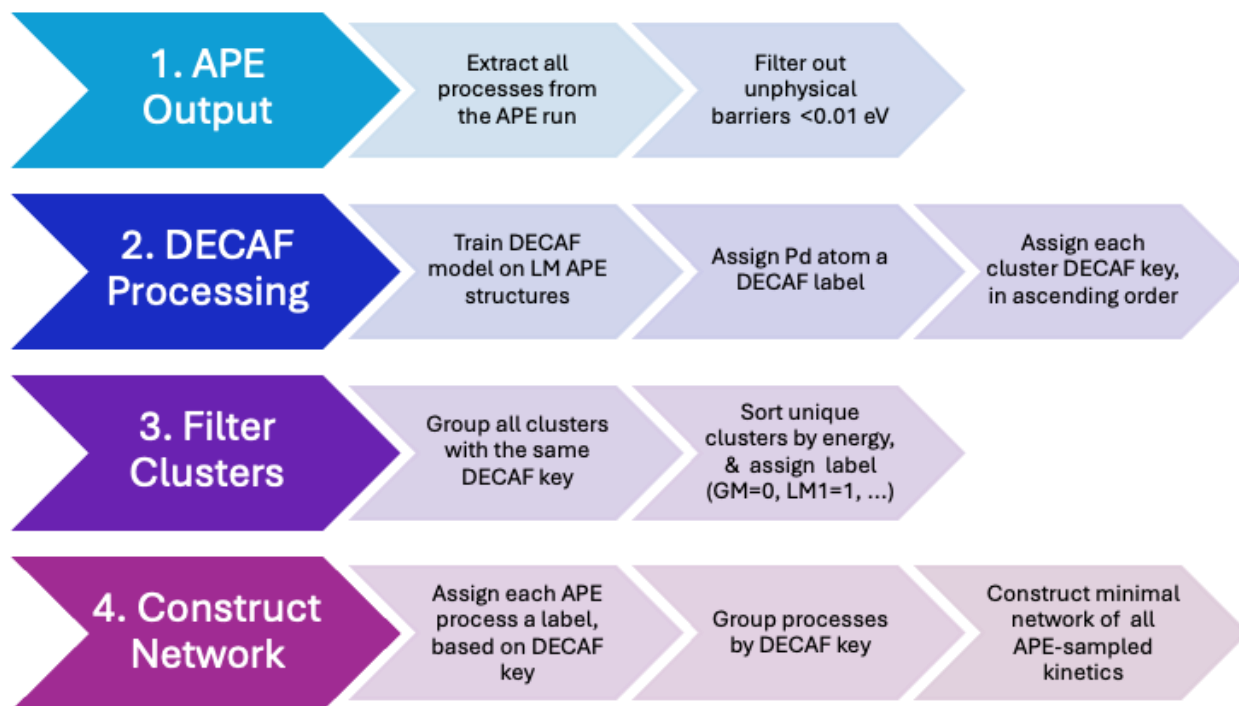
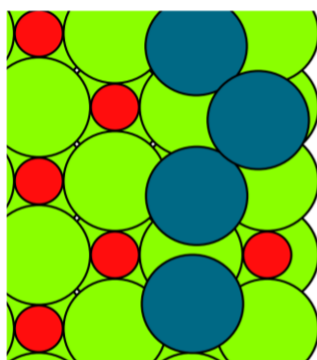


Figure S1. Flowchart summarizing the workflow for step (1) in Figure 2. This workflow using DECAF to take the APE library of elementary processes and convert them into the initial isomerization network.

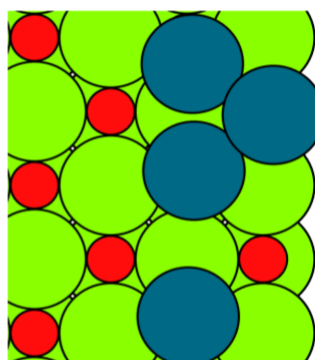
Supplemental Note 3: Merging and bypassing process for APE post-processing

Process (2) of Figure 2 involves the merging and bypassing of any nodes or states with barriers <0.1 eV leaving them. If there are two states which are separated by barriers in each direction than are <0.1 eV, then they are merged. An example for Pd₄/MgO is shown in Figure S2 below.

For this merging process, we then recalculate the barriers which entered the isomer which was eliminated relative to the isomer which was kept. Therefore, in the case for isomers 16 and 17 shown in Figure S2 above, if we had a process consisting of IS₁₇, TS₁₇, FS₁₇, we then recalculate the process starting from IS₁₆, using the total energies of TS₁₇ and FS₁₇ to calculate the new barrier.



Isomer 16
 ΔE_{GM} : 1.47 eV



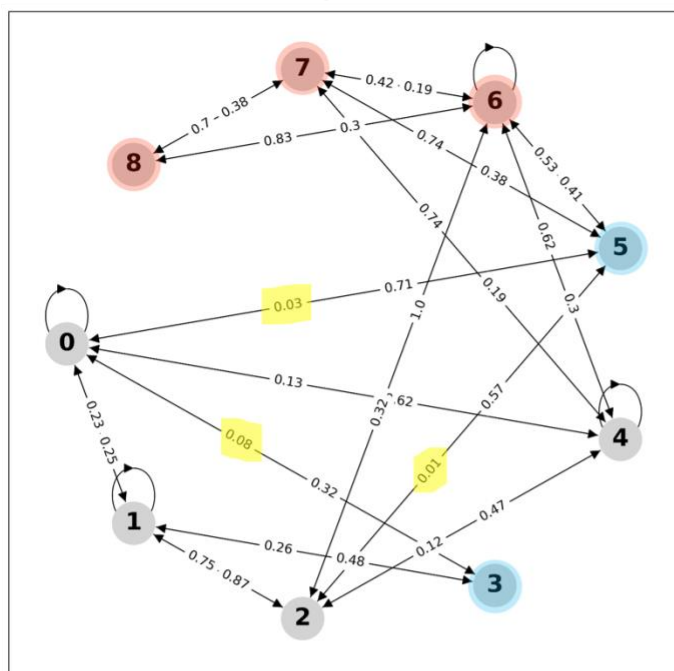
Isomer 17
 ΔE_{GM} : 1.53 eV

Figure S2. Two Pd4 structures which were separated by <0.1 eV barriers in each direction, which were merged into a single state.

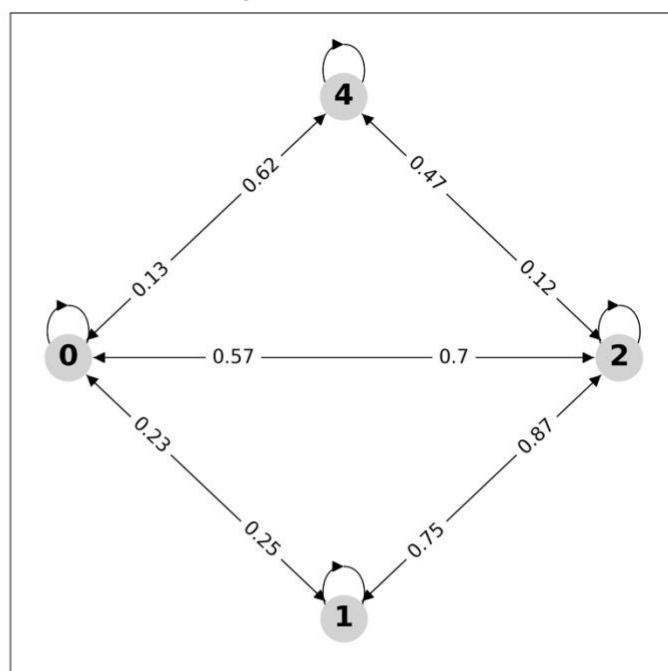
The bypassing process takes three states connected with two processes, and reduces it to two states connected with a single process, by eliminating the state in between the two final states. This is the state that has a process exiting it with a barrier <0.1 eV, which is however >0.1 eV in the opposite direction. In order to maintain detailed balance, and ensure that the rates are calculated correctly, the barrier between the two final states is taken using the TS structure with the highest energy for the process, and use that as the TS between the new initial and final states.

In addition to this merging and bypassing, we eliminate any structures which result in the fragmentation of the cluster. While this is a vital process when considering the sintering and/or redispersion of clusters, it is not the focus of the current work. Figures S3 and S4 show visual representations of the reduction of the isomerization network for Pd3 and Pd4 into the final version which are shown in the main text.

(a) Unreduced Network: Pd₃/MgO



Final Network: Pd₃/MgO

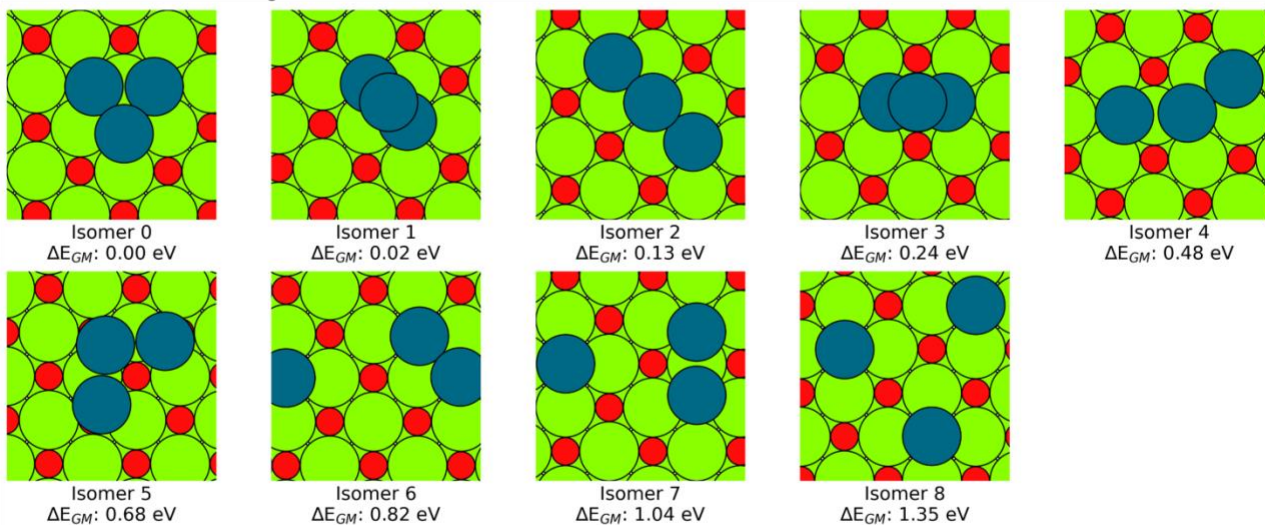


Fragmented clusters- removed

Bypassed clusters- removed

Merged clusters- combined

(b) Unreduced Pd₃ Ensemble



(c) Reduced Pd₃ Ensemble

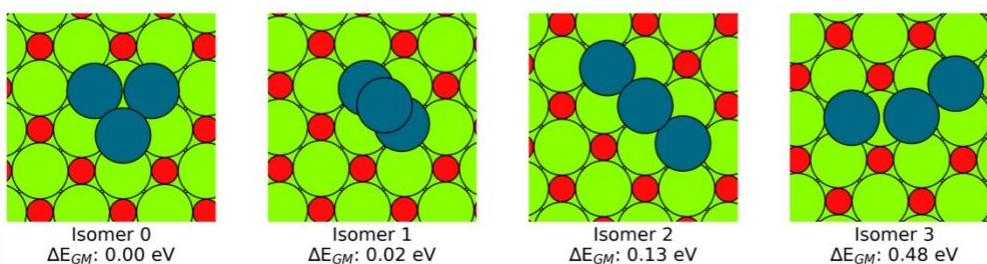
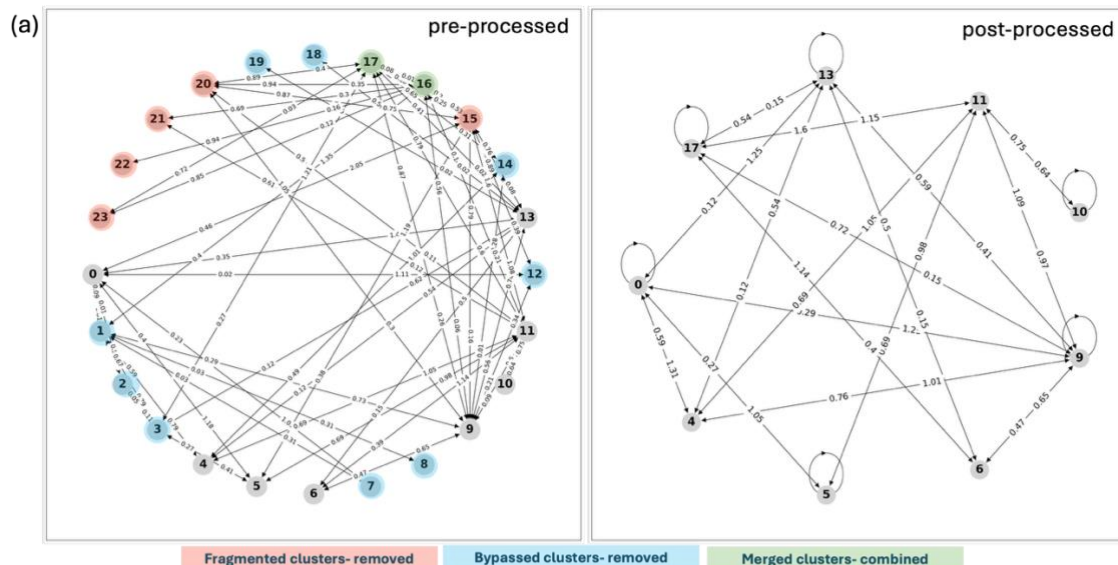
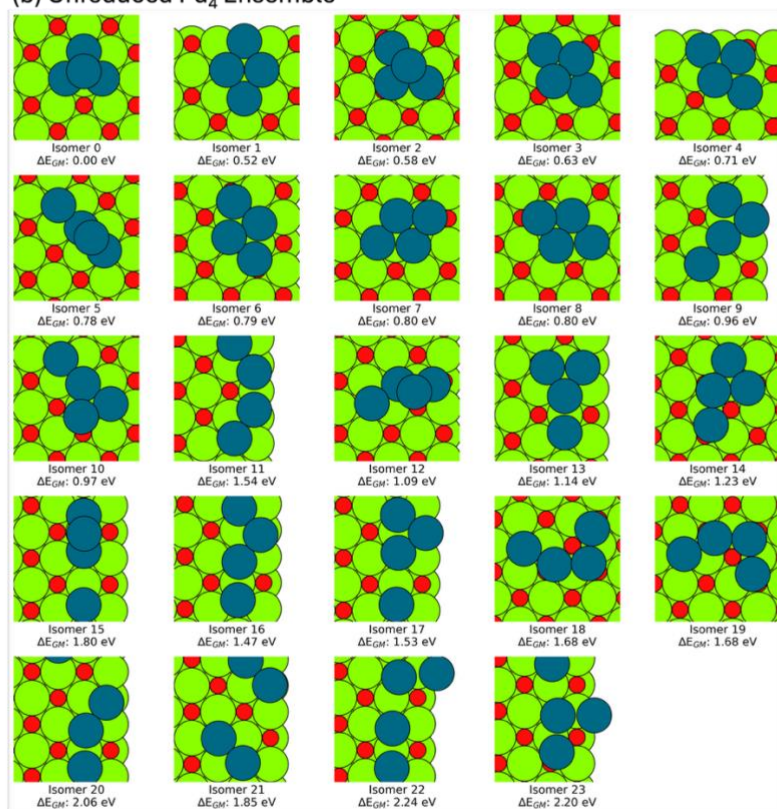


Figure S3. Comparison of Pd₃/MgO network (a) before (left) and after (right) reduction, where fragmented clusters (in red), and states with barriers < 0.1 eV exiting them (in blue) are removed from the final network. (b) shows the unreduced network, and (c) shows the final network, after removal of fragmented clusters, and structures which were determined to be dynamically unstable.



(b) Unreduced Pd₄ Ensemble



(c) Reduced Pd₄ Ensemble

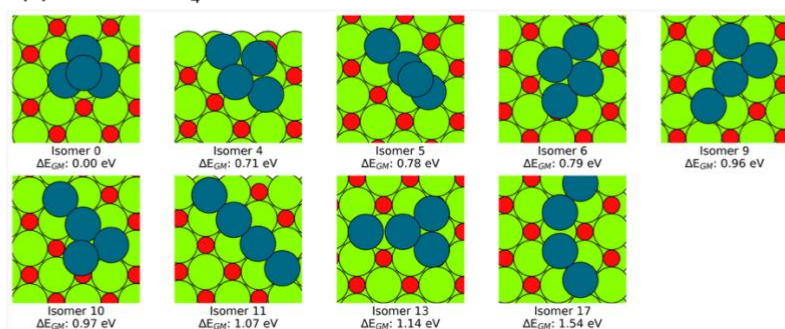


Figure S4. Comparison of Pd₄/MgO network (a) before (left) and after (right) reduction, where fragmented clusters (in red), and states with barriers <0.1 eV exiting them (in blue) are removed from the final

network. States which are merged (barriers <0.1 eV both directions) are shown in green. (b) shows the unreduced ensemble of structures, and (c) shows the final ensemble of structures, after removal of fragmented clusters, and structures which were determined to be dynamically unstable.

Supplementary Note 4: Construction of a the rate matrix for dynamics simulations.

To explore the dynamics of the isomerization networks for each cluster size, we need to construct a rate matrix that contains all information about the transitions between all states. To start, we need to convert the barriers for each process into an associated rate. This is done using harmonic transition state theory (hTST).

$$k_{ij} = A e^{-\Delta E_a/k_B T}$$

Where k_{ij} is the rate of going from state i to state j , where the activation energy barrier is ΔE_a . The preexponential factor A is calculated directly from APE, rather than assuming that $A = k_B T/h$.

We calculate the rates for all barriers in a given reaction network. From these, we then construct the rate matrix, or left stochastic matrix, using the format outlined in Figure S5 below.

	1	2	3	(... N)
1	$-\sum_i k_{i \rightarrow 1}$	$k_{1 \rightarrow 2}$	$k_{1 \rightarrow 3}$	(...) $k_{1 \rightarrow N}$
2	$k_{2 \rightarrow 1}$	$-\sum_i k_{i \rightarrow 2}$	$k_{2 \rightarrow 3}$...
3	$k_{3 \rightarrow 1}$	$k_{3 \rightarrow 2}$	$-\sum_i k_{i \rightarrow 3}$...
(... N)	(...) $k_{N \rightarrow 1}$	(...) $-\sum_i k_{i \rightarrow N}$

Figure S5. Construction of a rate matrix for a system with N states. Off-diagonal states represent the total rate entering a given state. On-diagonal states are the negative sum of all processes entering a state.

Note that k_{ij} does not represent here a single kinetic process, but is in fact the sum of all rates for that process; APE sampling gives us multiple transition states between the same two endpoints (see Figure S6 for examples for Pd_3). While these can be very different, and are theoretically dominated only by the processes with the lowest barriers, we include all of them for completeness.

Using this rate matrix, we can evaluate its dynamics in two different ways. The first, and simplest, is to obtain the eigenvalues and associated eigenvectors from the rate matrix. The first eigenvalue, $\lambda_1 \cong 0$, and the associated vector \mathbf{v}_1 , when normalized, gives the steady-state populations after an infinite relaxation time. This should be equivalent to the Boltzmann populations; in order for this to be accurate, we must use arbitrary precision in our calculations, as our calculated rates vary by 10+ orders of magnitude. The second eigenvalue λ_2 can be used to estimate the timescale required for the system to relax to thermal equilibrium, via $\tau_{rel} = -\frac{1}{\lambda_2}$. To confirm these values, we also explore the evolution of isomer populations using the matrix exponential approach. The change of state population with time can be represented as

$$\frac{d}{dt}p_i = \sum_j w_{ij}p_j - \sum_j w_{ji}p_i$$

We can then represent the evolution of the populations of each isomer as

$$\frac{d}{dt}\bar{P} = \hat{G} \cdot \bar{P}$$

From which we can then take the matrix exponential to explore the evolution of the system state populations (P) with time, starting from a specific initial configuration at $t=0$ ($P_{t=0}$)

$$\bar{P} = e^{t \cdot \hat{G}} \bar{P}_{t=0}$$

Where G is the rate matrix outlined above.

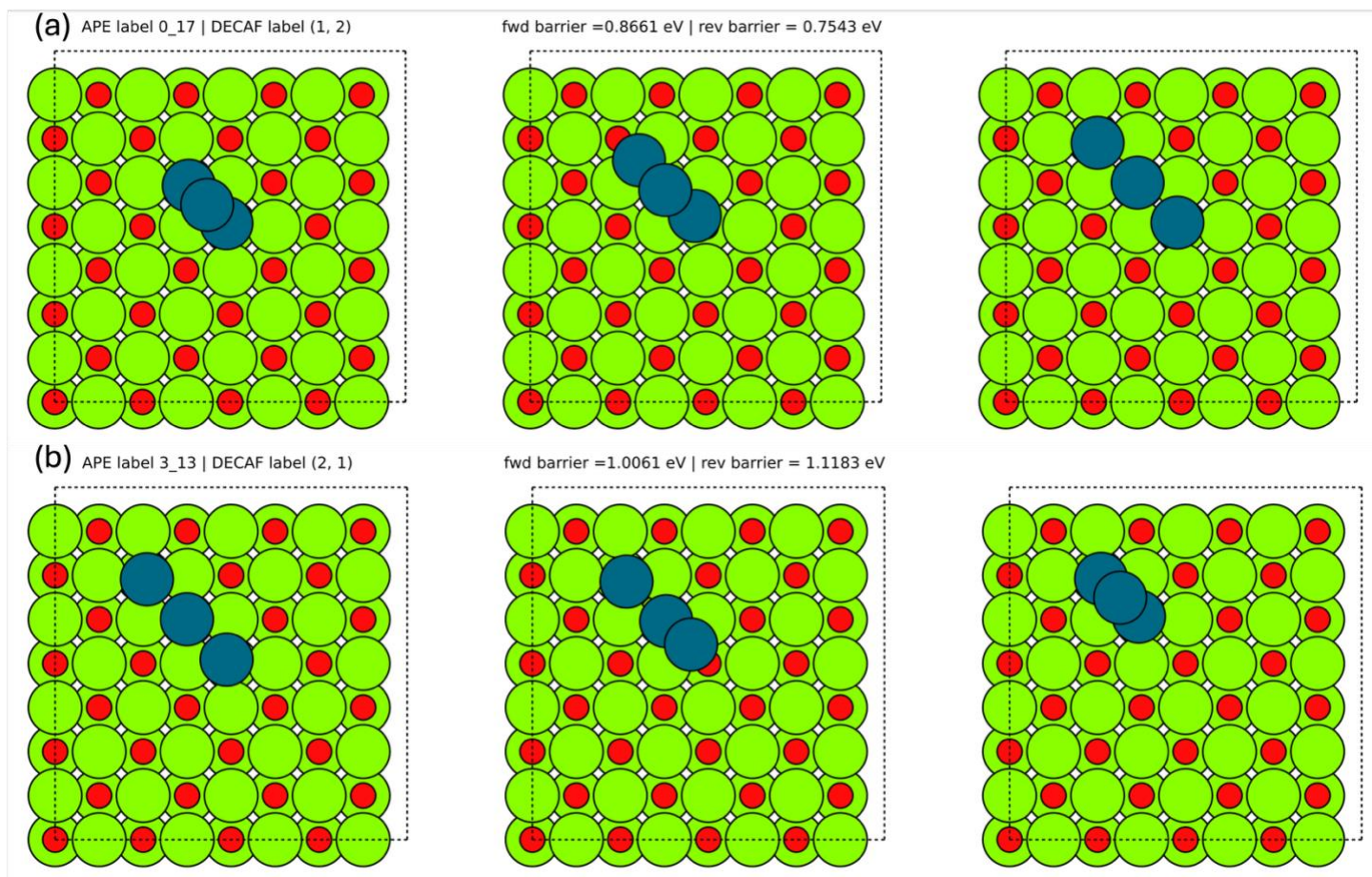


Figure S6. Examples of two different barriers for the restructuring between isomers 1 and 2. Note that depending on which atom moves, and how they move, the barrier can be significantly different.

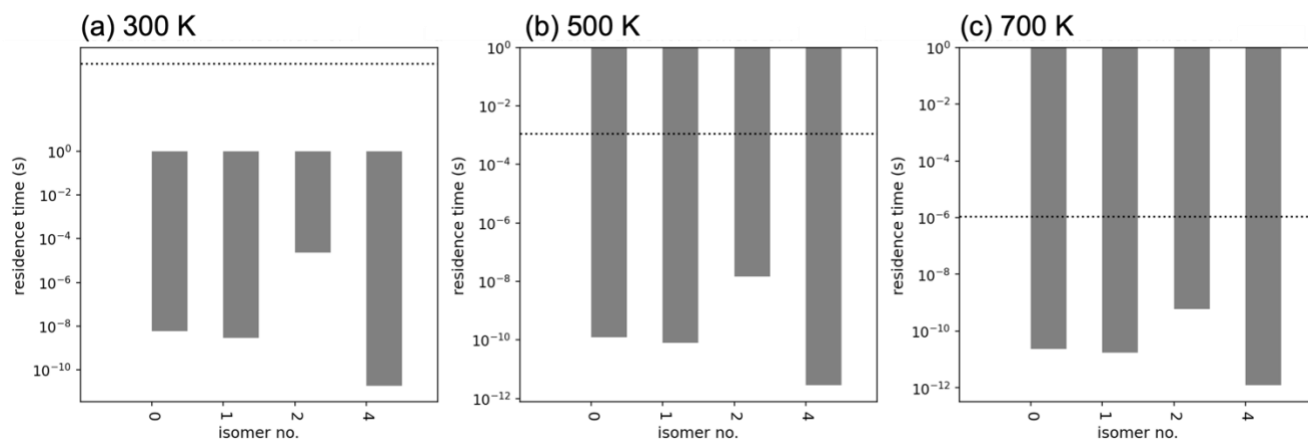


Figure S7. Histograms of residence times for Pd3 for (a) 300 K (b) 500 K and (c) 700K. The horizontal dashed line represents the rate required to overcome a 1 eV barrier at the given temperature .

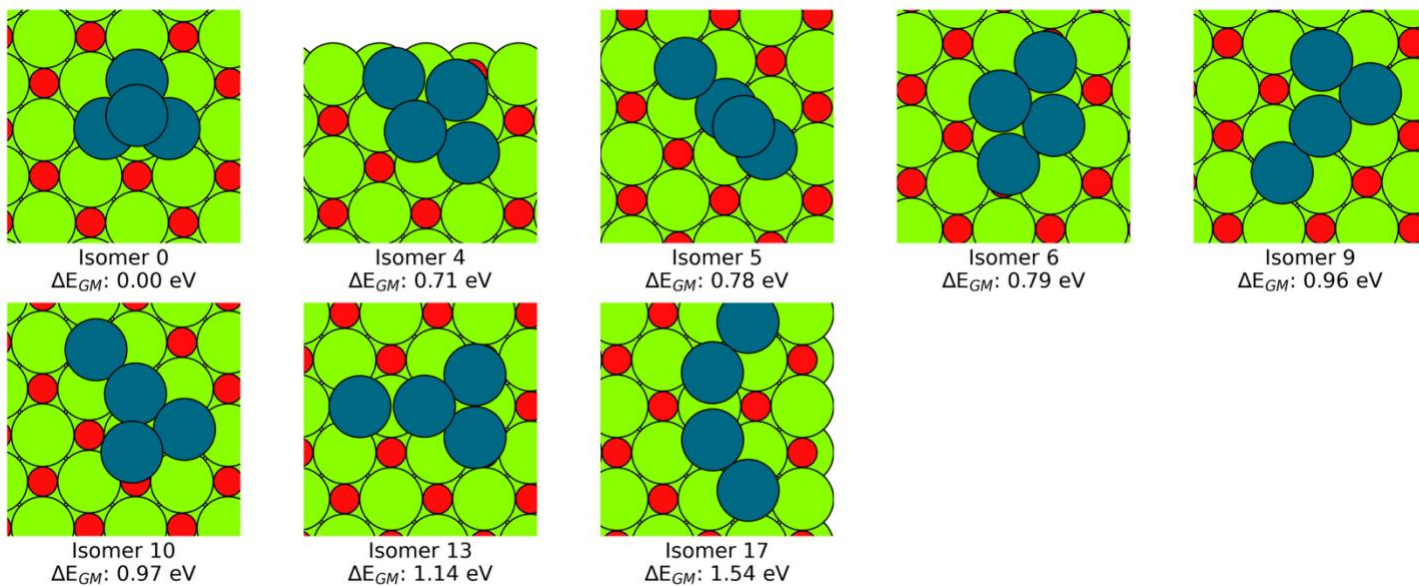


Figure S8. Ensemble of structures for Pd4

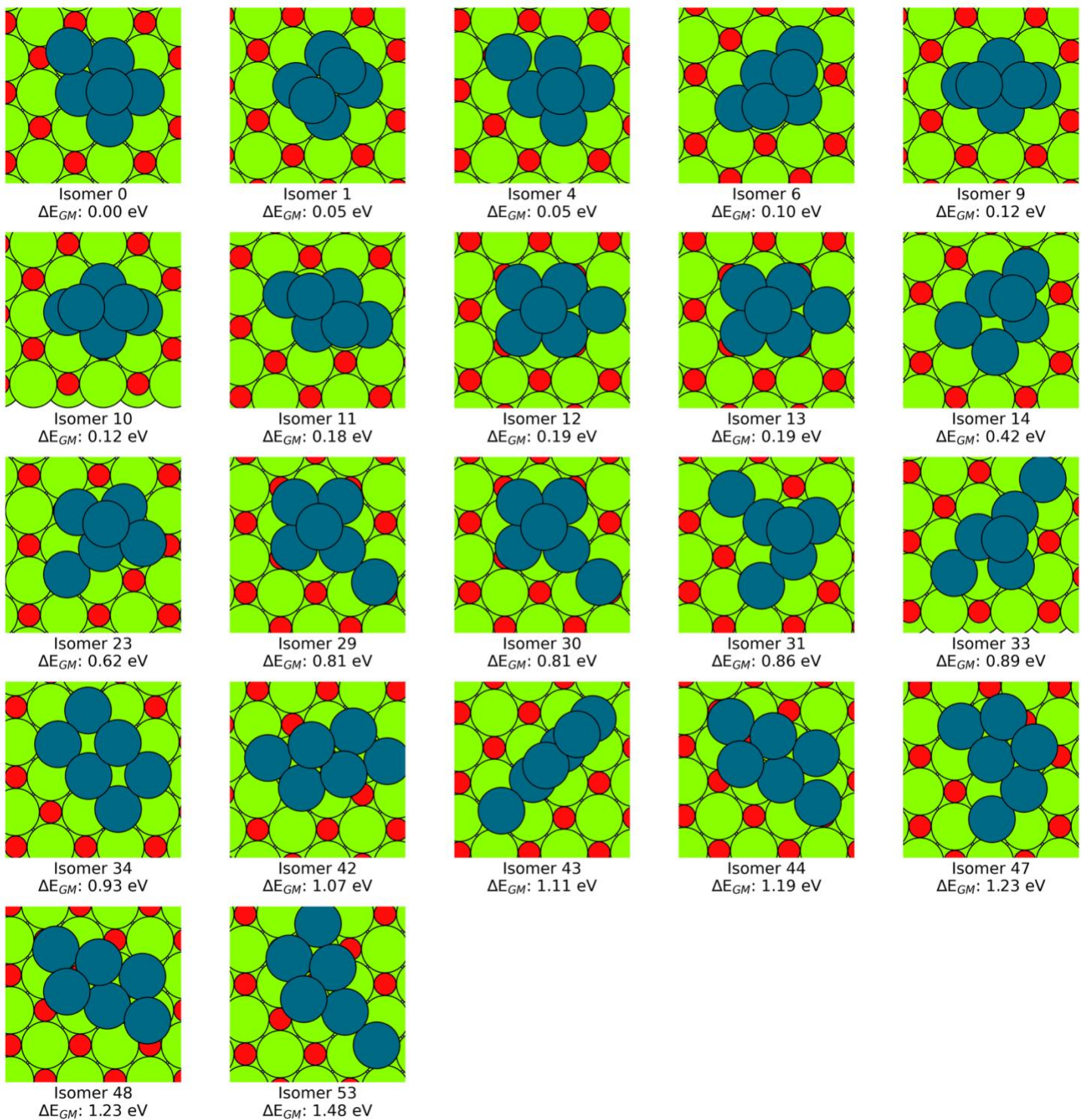


Figure S9. Ensemble of structures for Pd6

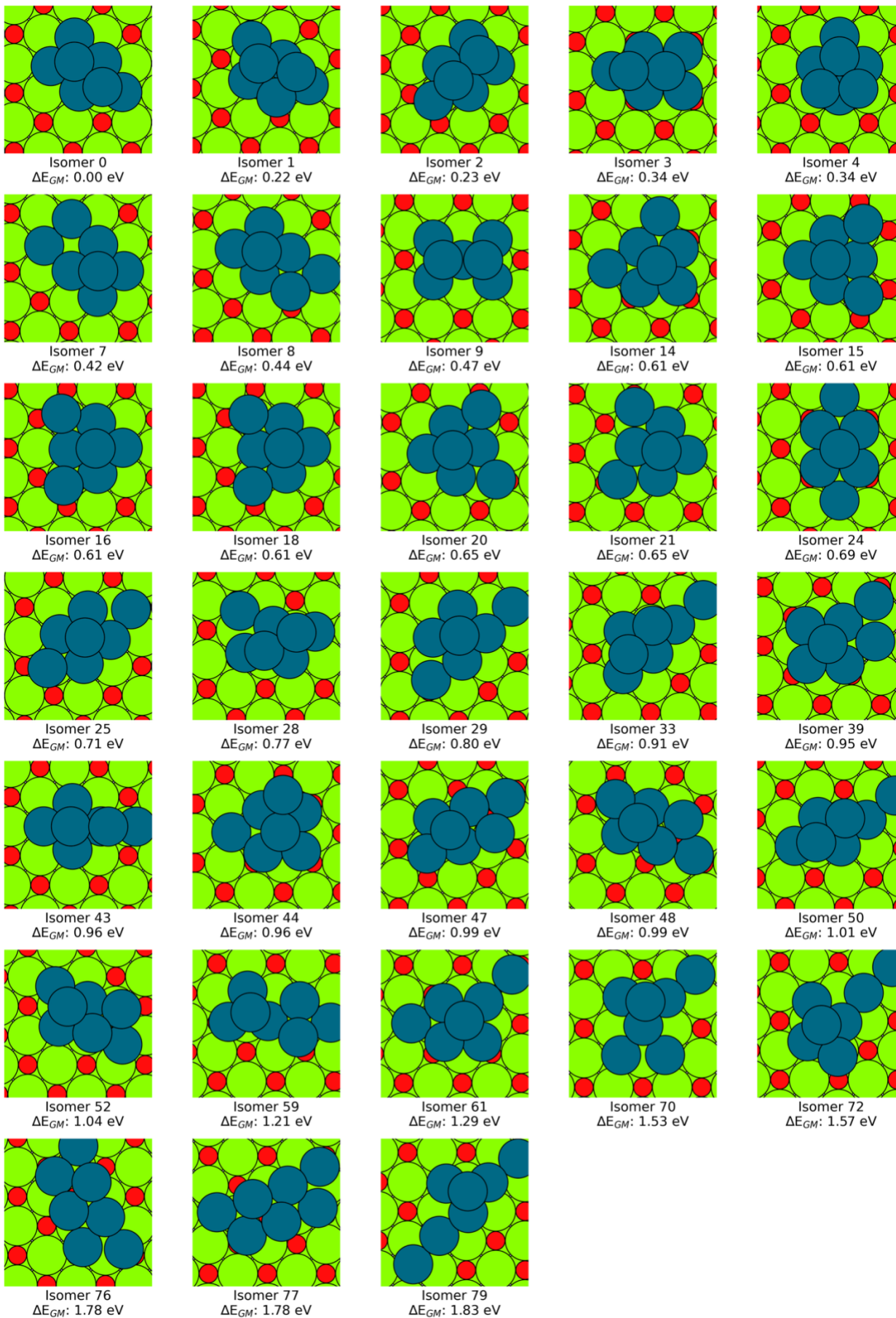
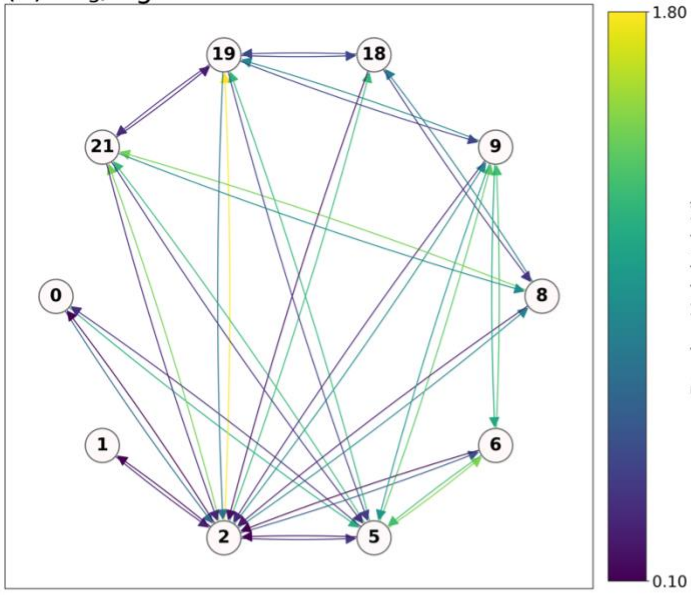
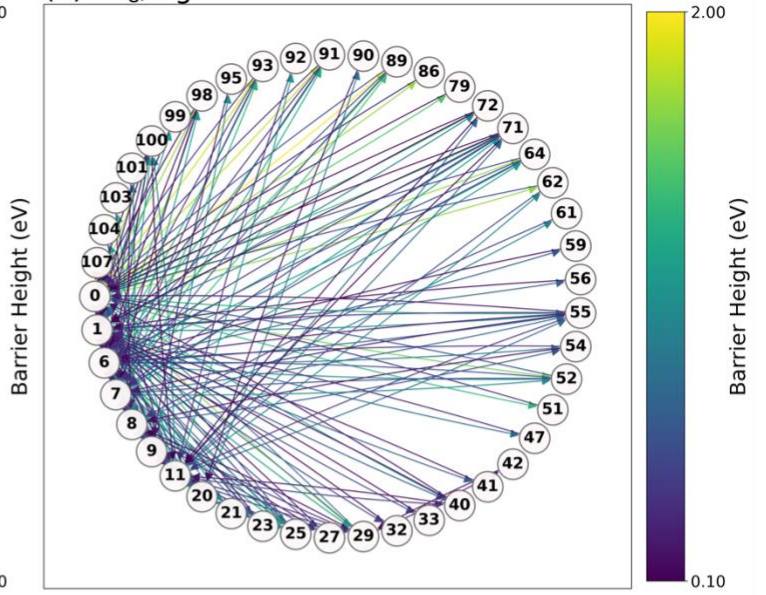


Figure S10. Ensemble of structures for Pd7

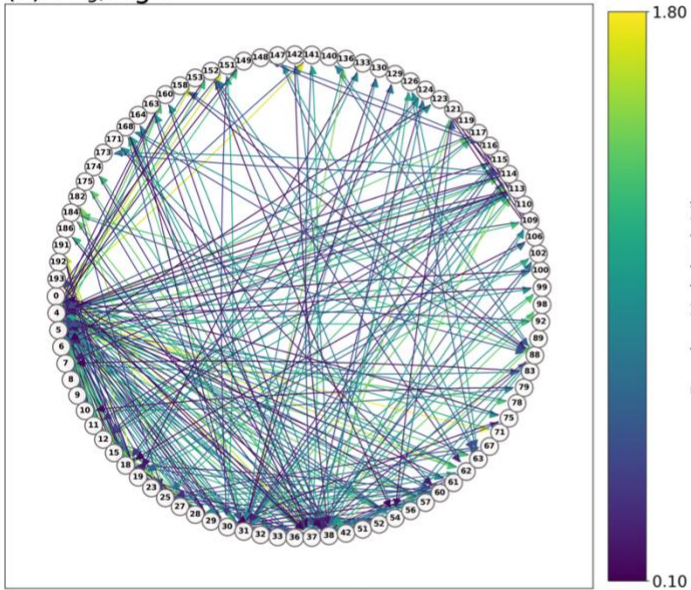
(a) Pd₅/MgO



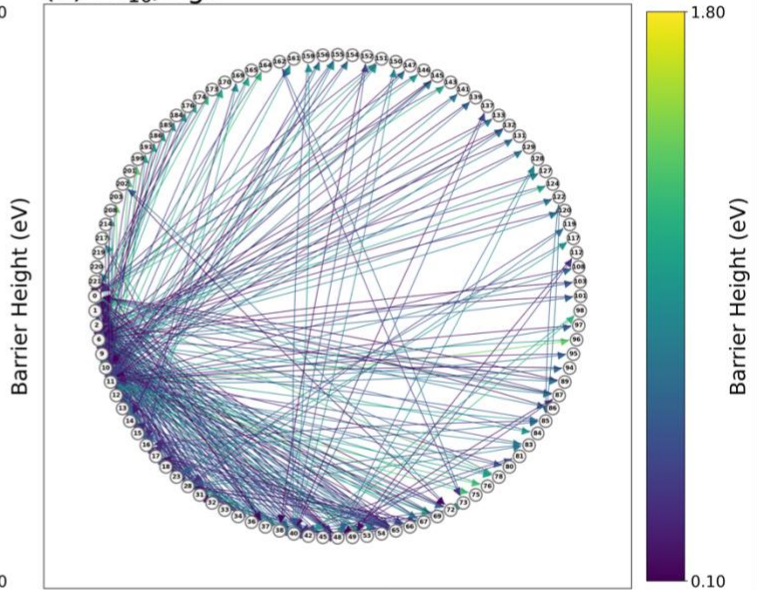
(b) Pd₈/MgO



(c) Pd₉/MgO



(d) Pd₁₀/MgO



(e) Pd₁₁/MgO

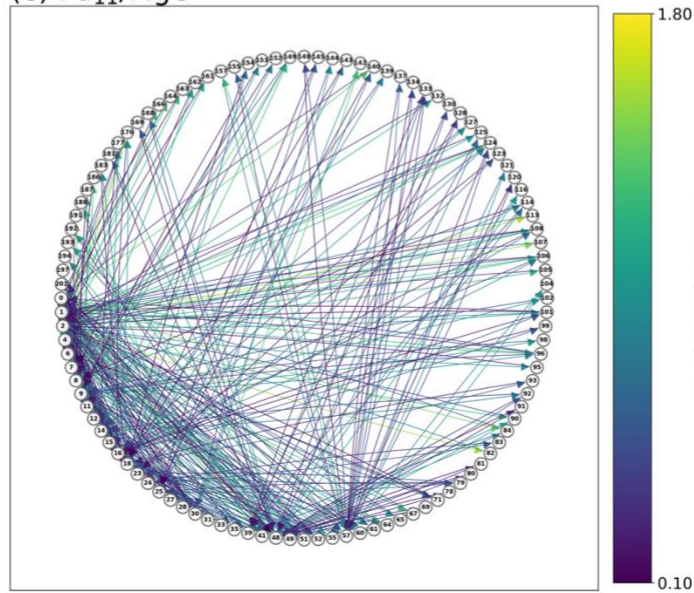


Figure S11. Remaining isomerization networks; Pd5, Pd8, Pd9, Pd10, and Pd11.

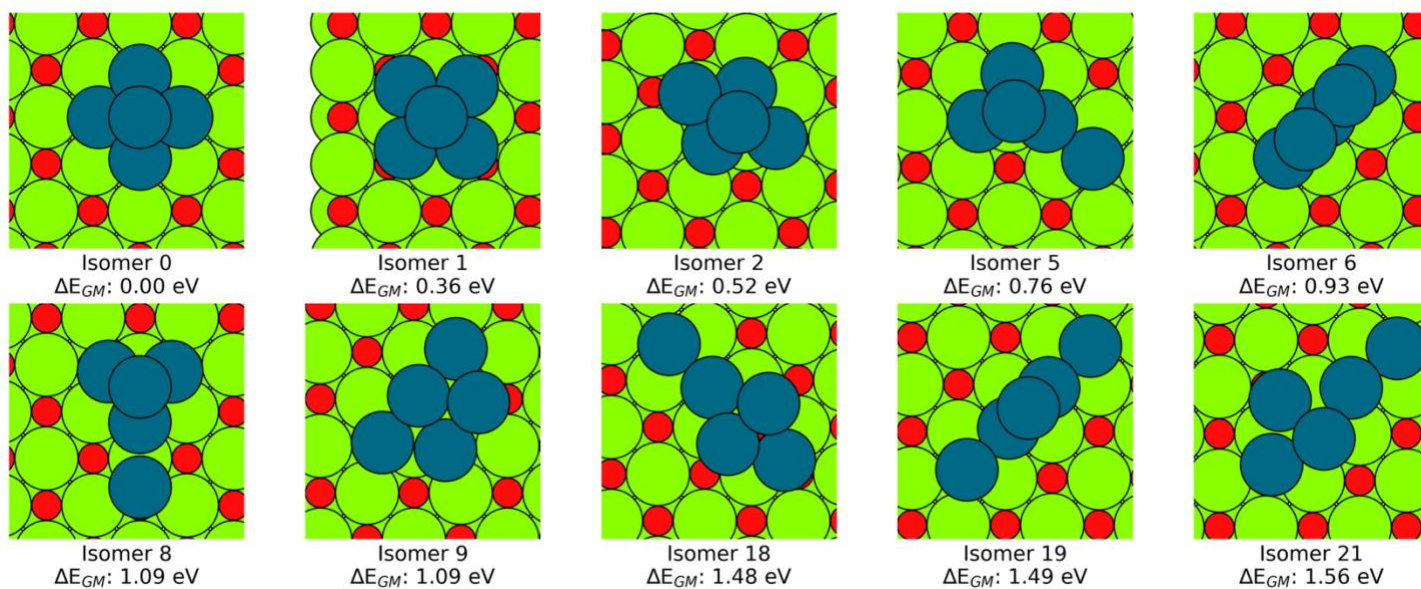


Figure S12. Ensemble of structures for Pd5

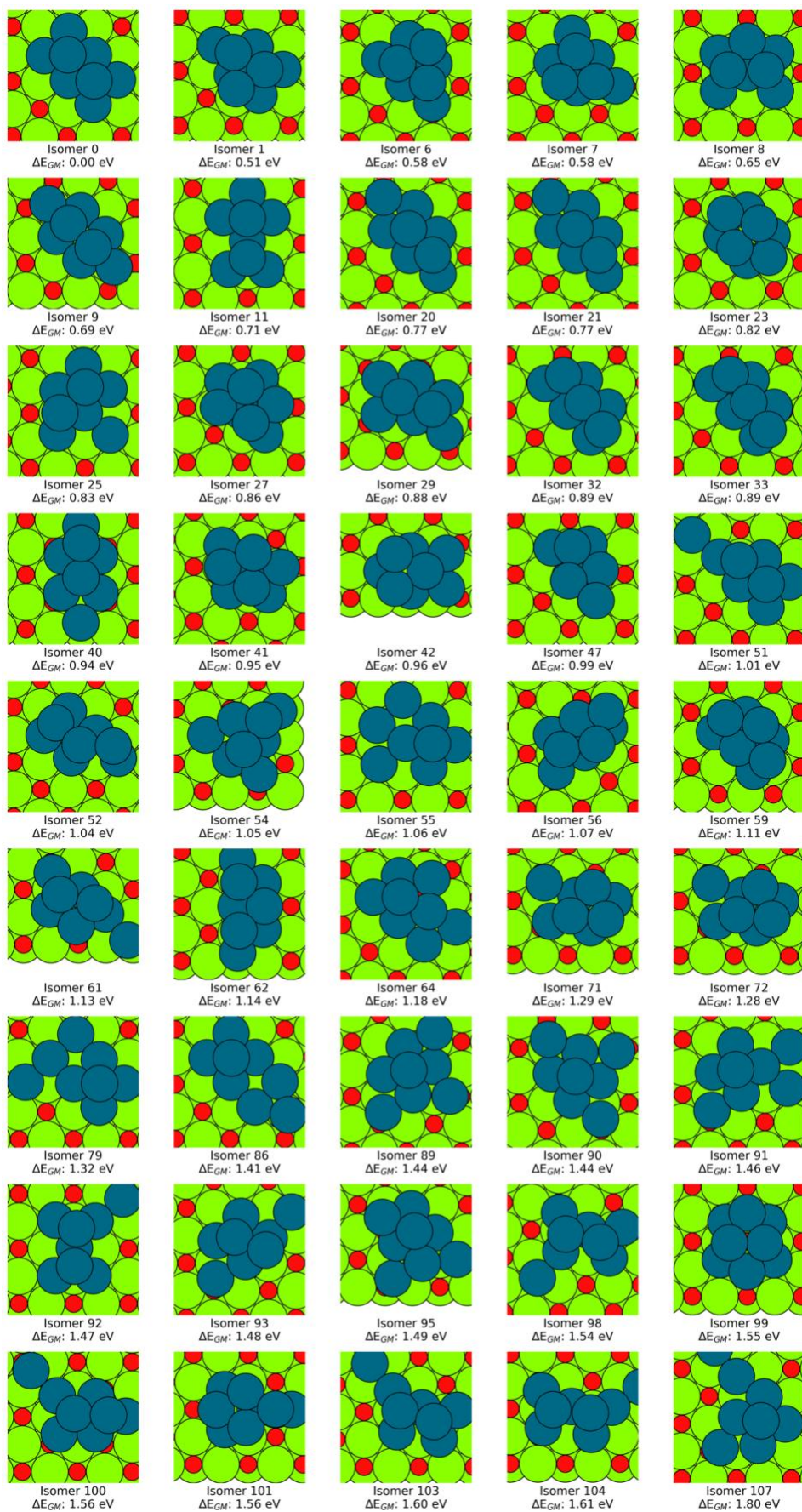


Figure S13. Ensemble of structures for Pd8

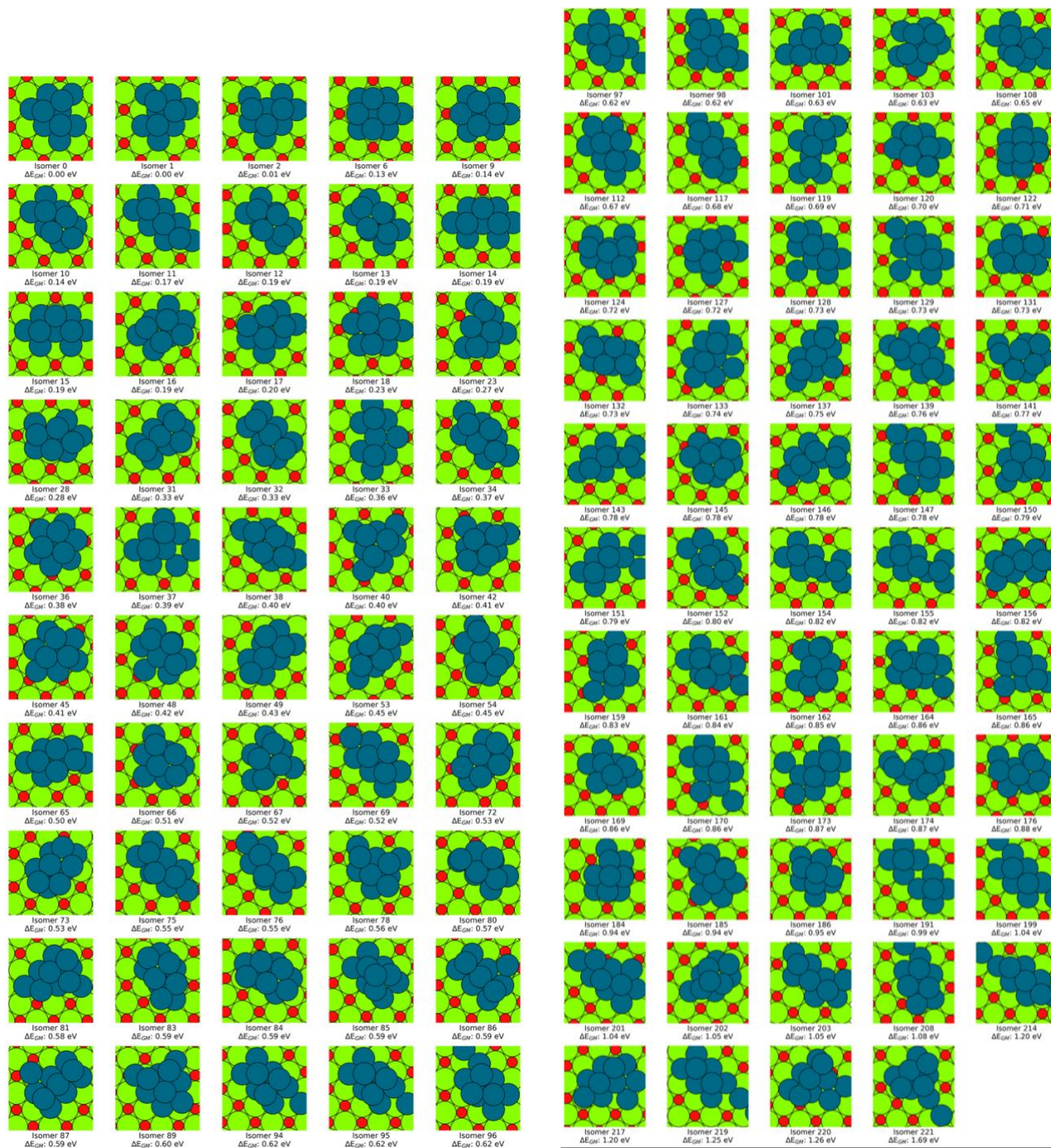


Figure S15. Ensemble of structures for Pd₁₀

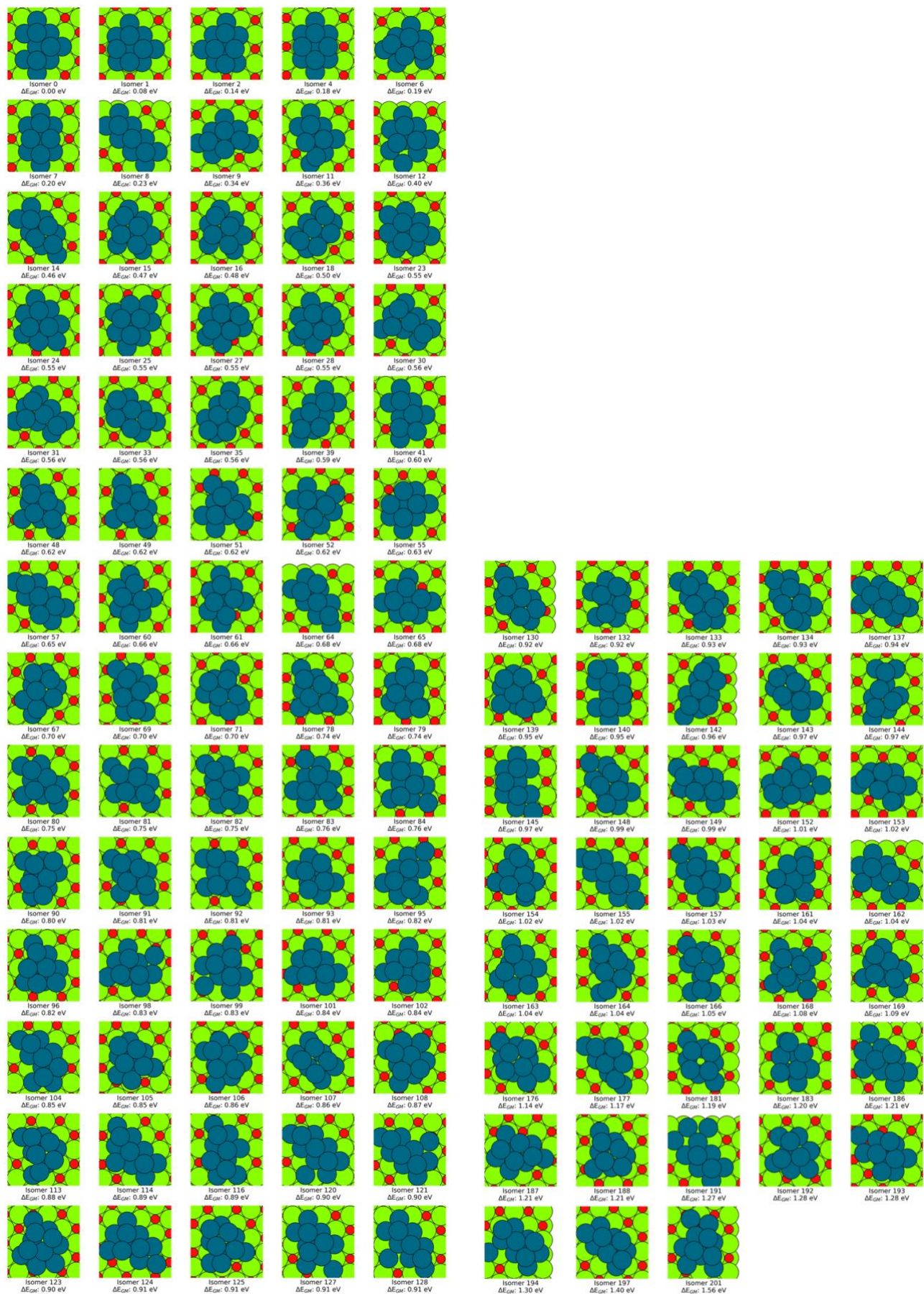


Figure S16. Ensemble of structures for Pd11

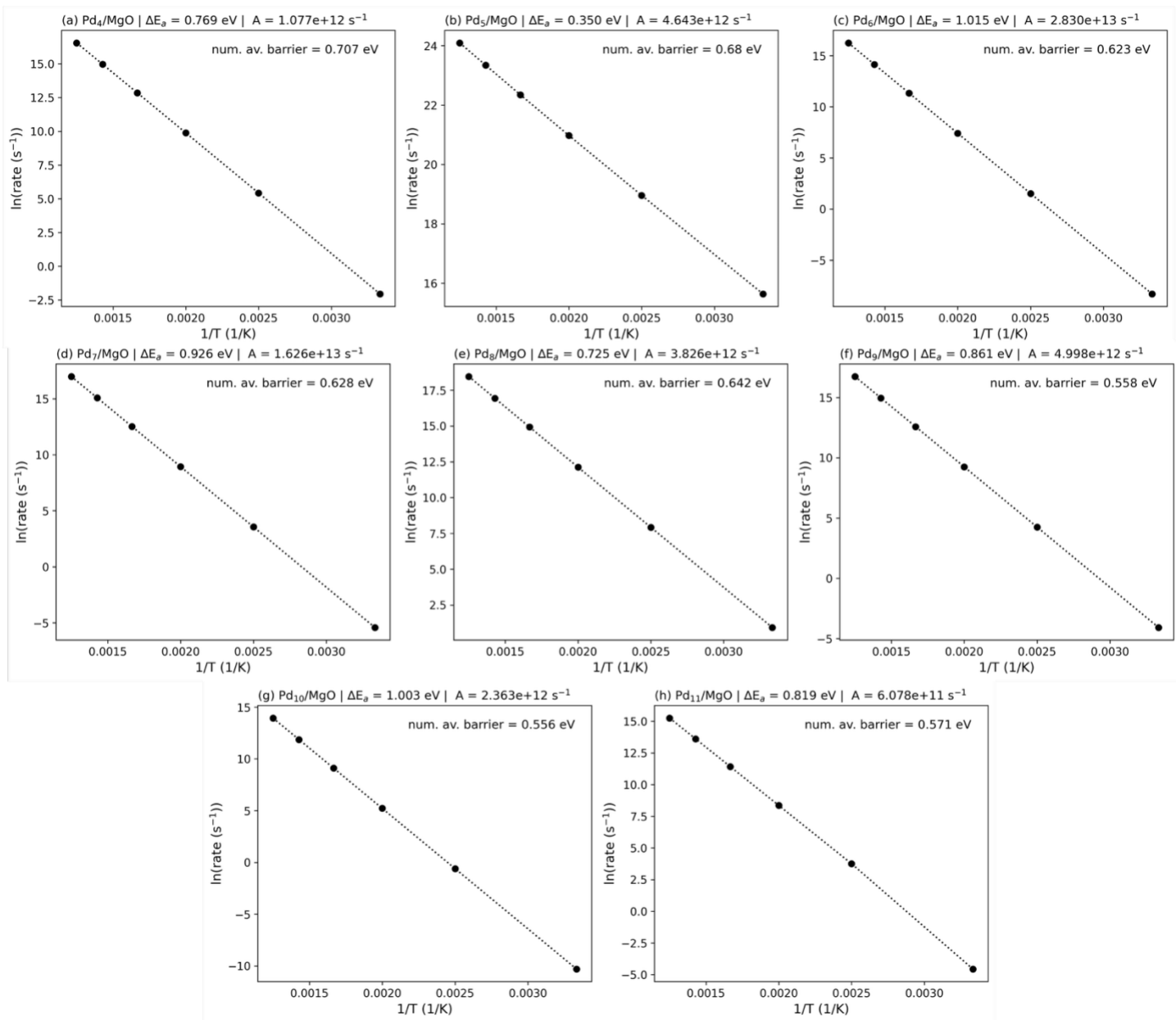


Figure S17. Arrhenius plots for all cluster sizes

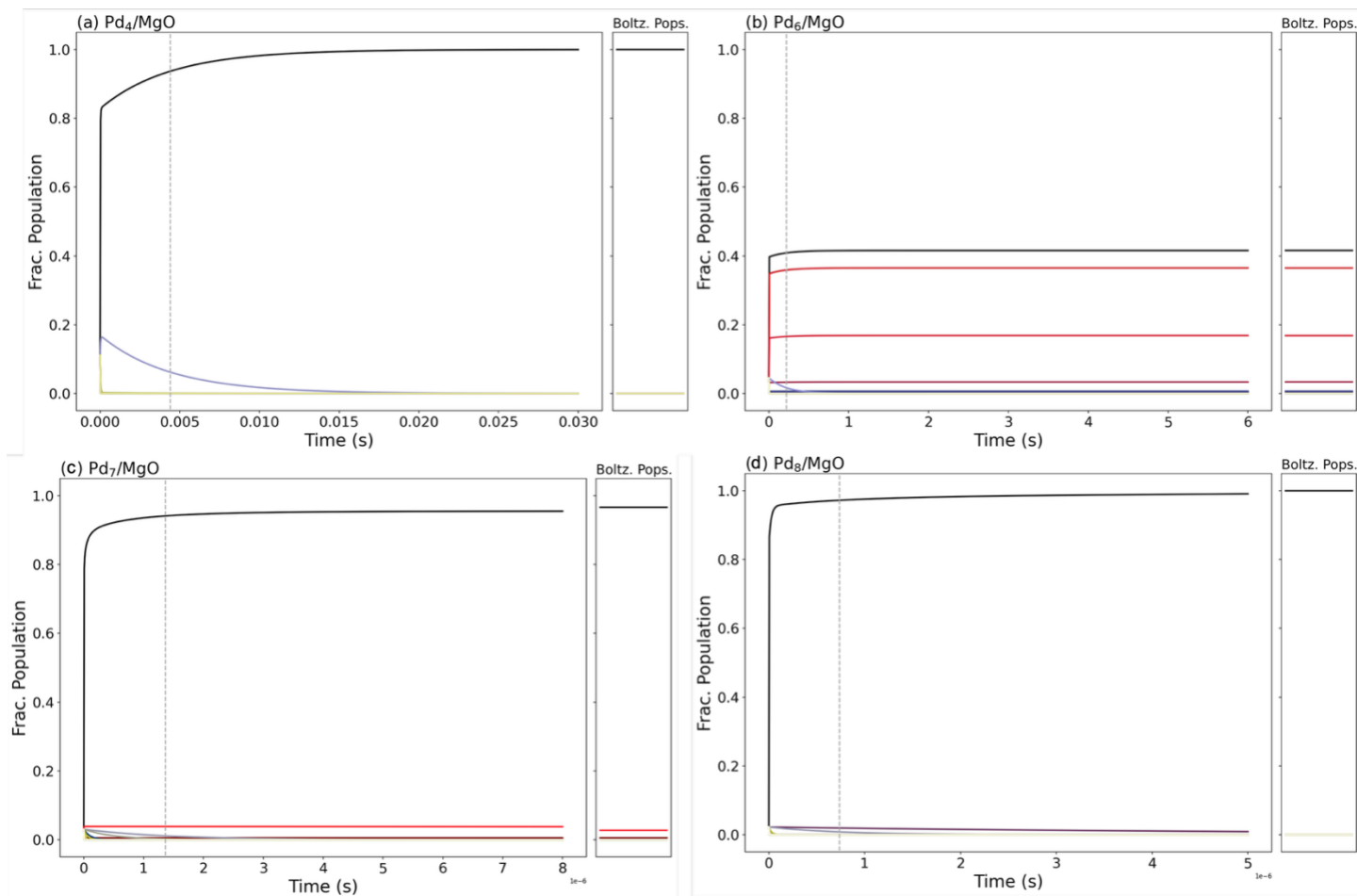


Figure S18. Matrix Exponential plots for (a) Pd₄/MgO, (b) Pd₆/MgO, (c) Pd₇/MgO and (d) Pd₈/MgO

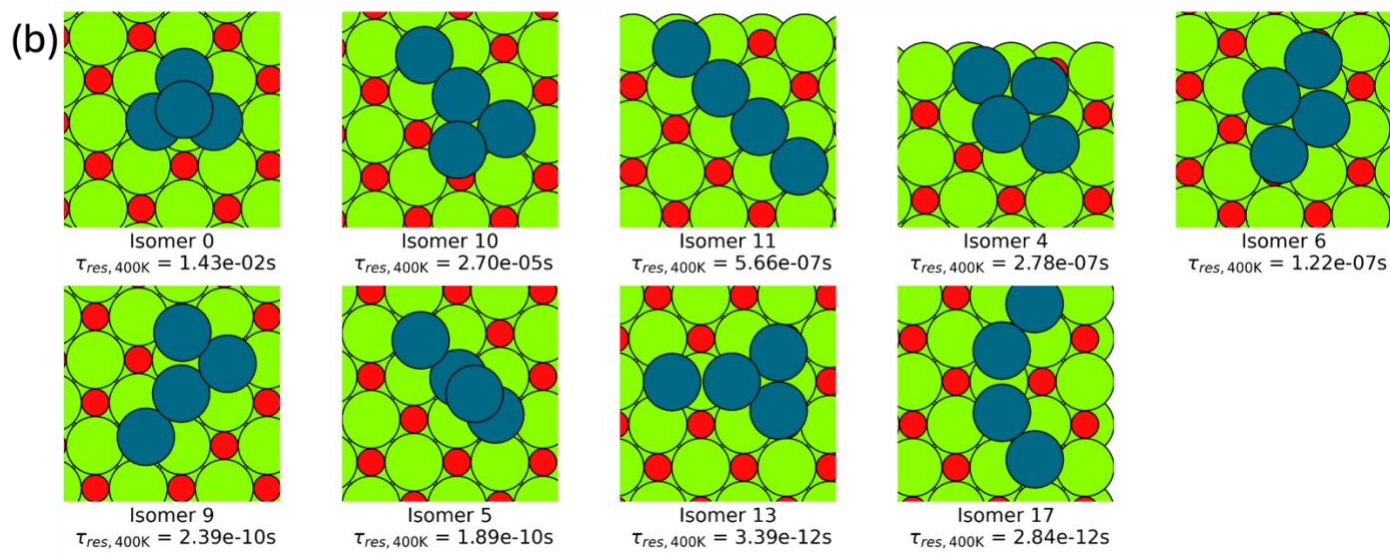
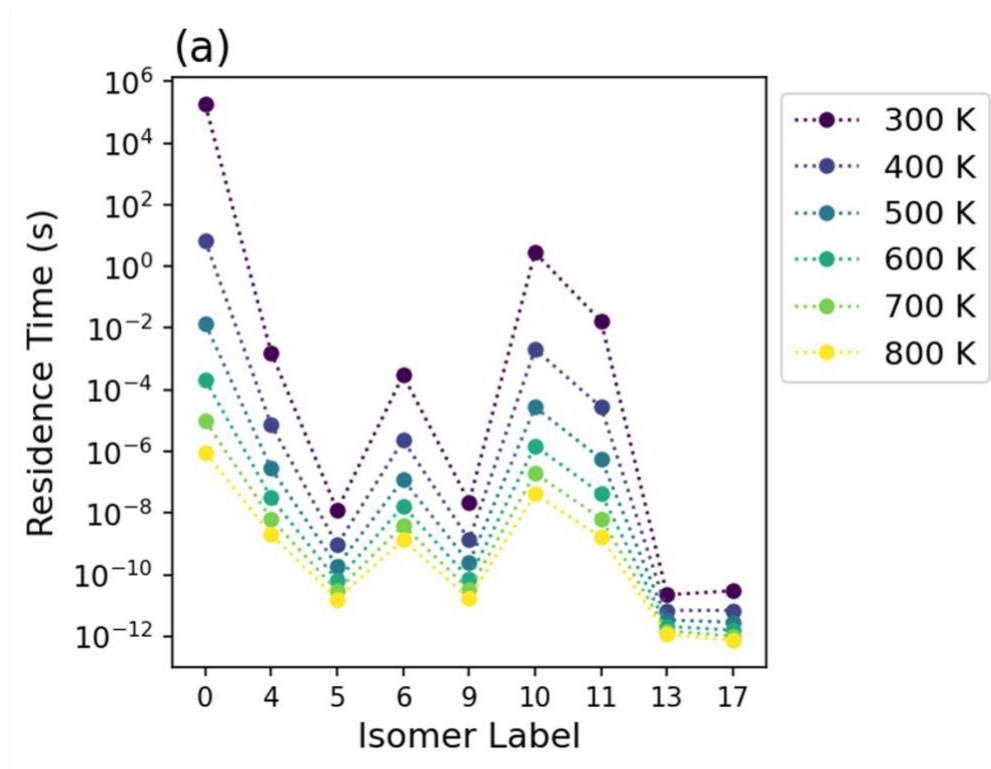


Figure S19. Pd4 residence time and top 5 dynamically stable structures

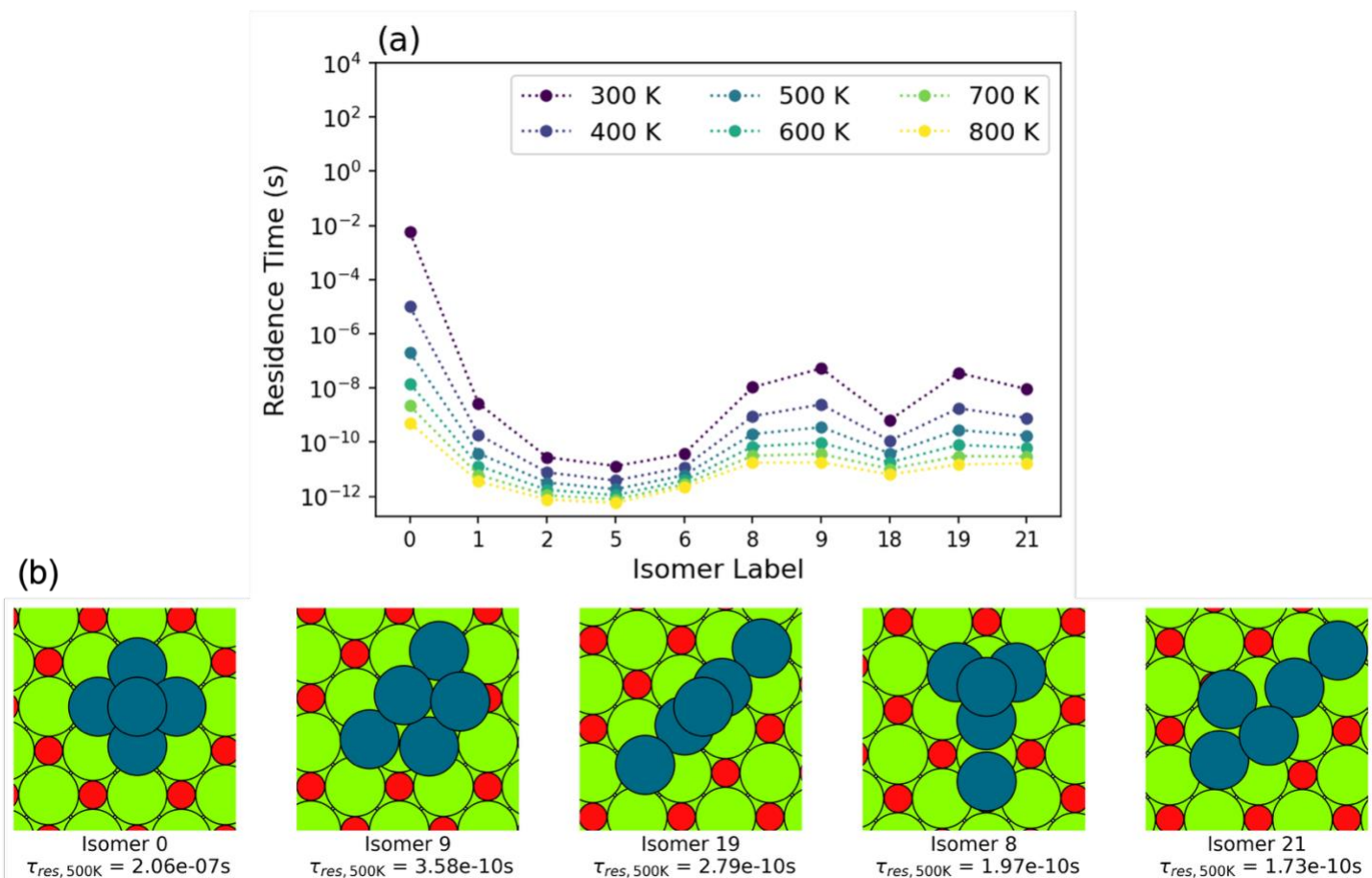


Figure S20. Pd5 residence time and top 5 dynamically stable structures

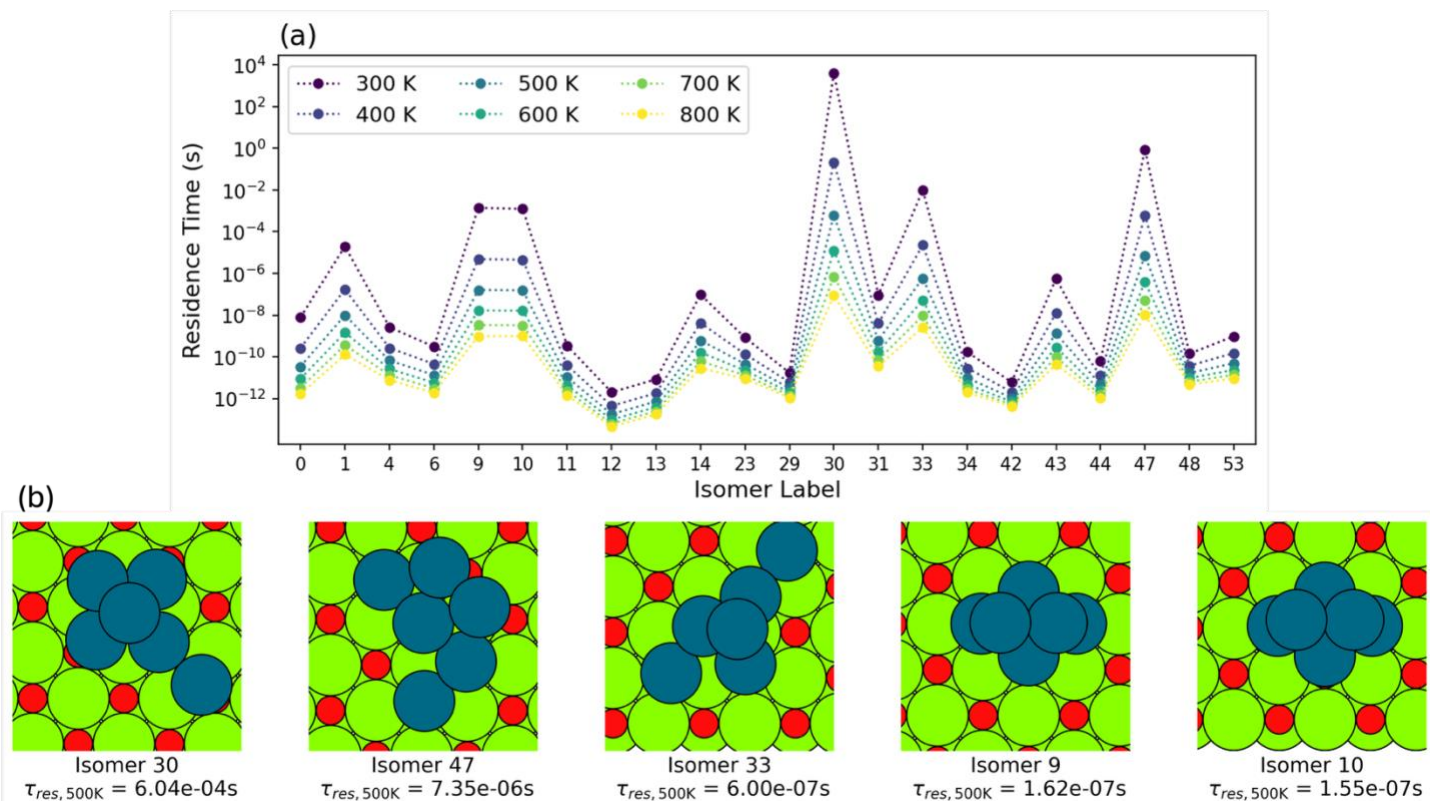


Figure S21. Pd6 residence time and top 5 dynamically stable structures

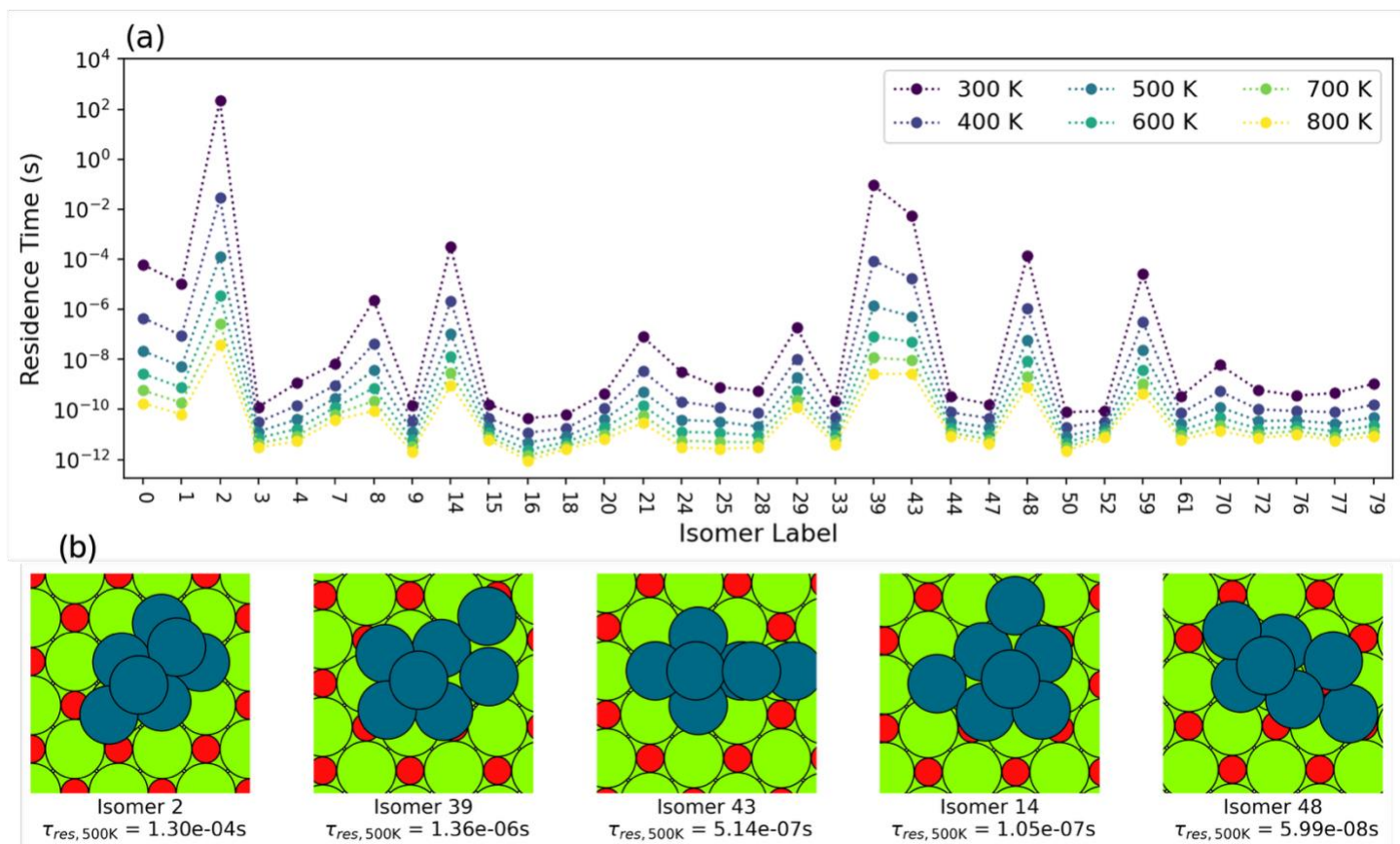


Figure S22. Pd7 residence time and top 5 dynamically stable structures

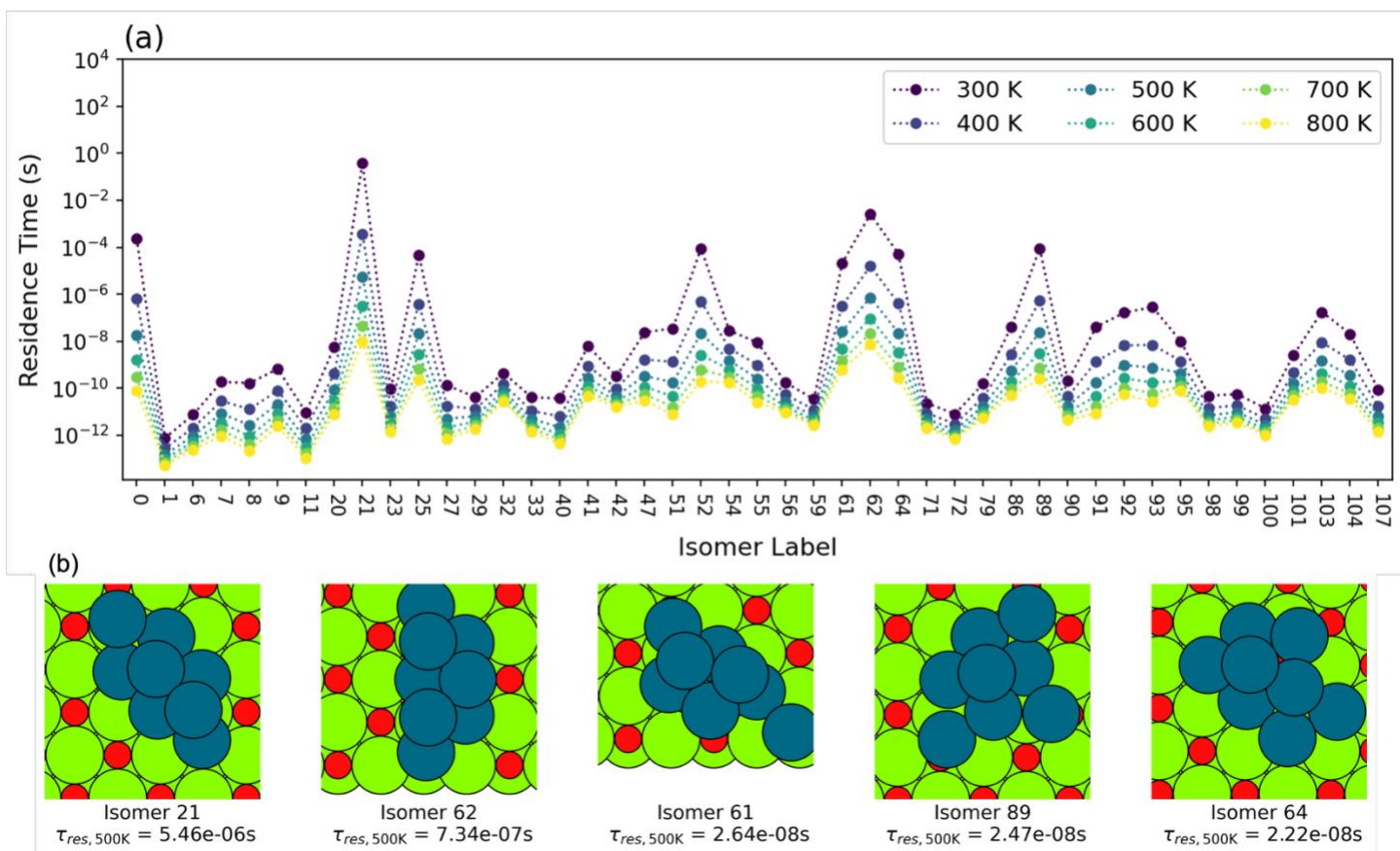


Figure S23. Pd8 residence time and top 5 dynamically stable structures

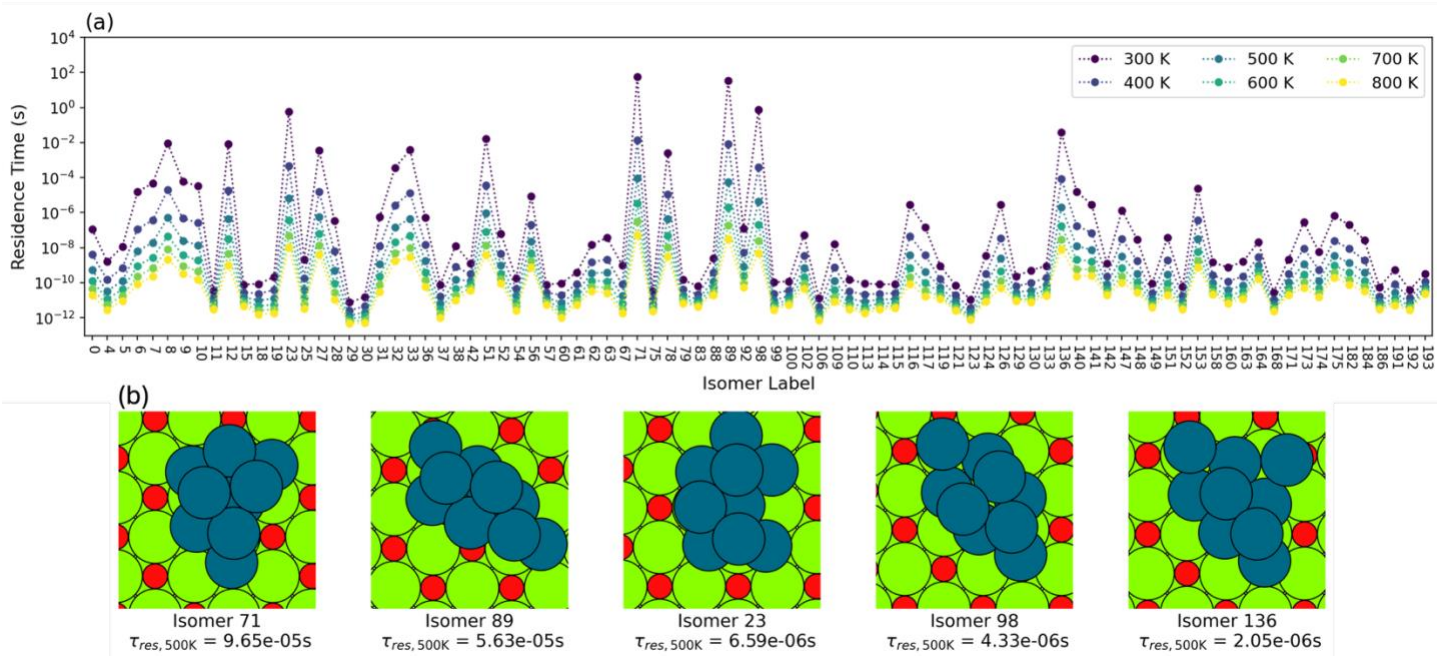


Figure S24. Pd9 residence time and top 5 dynamically stable structures

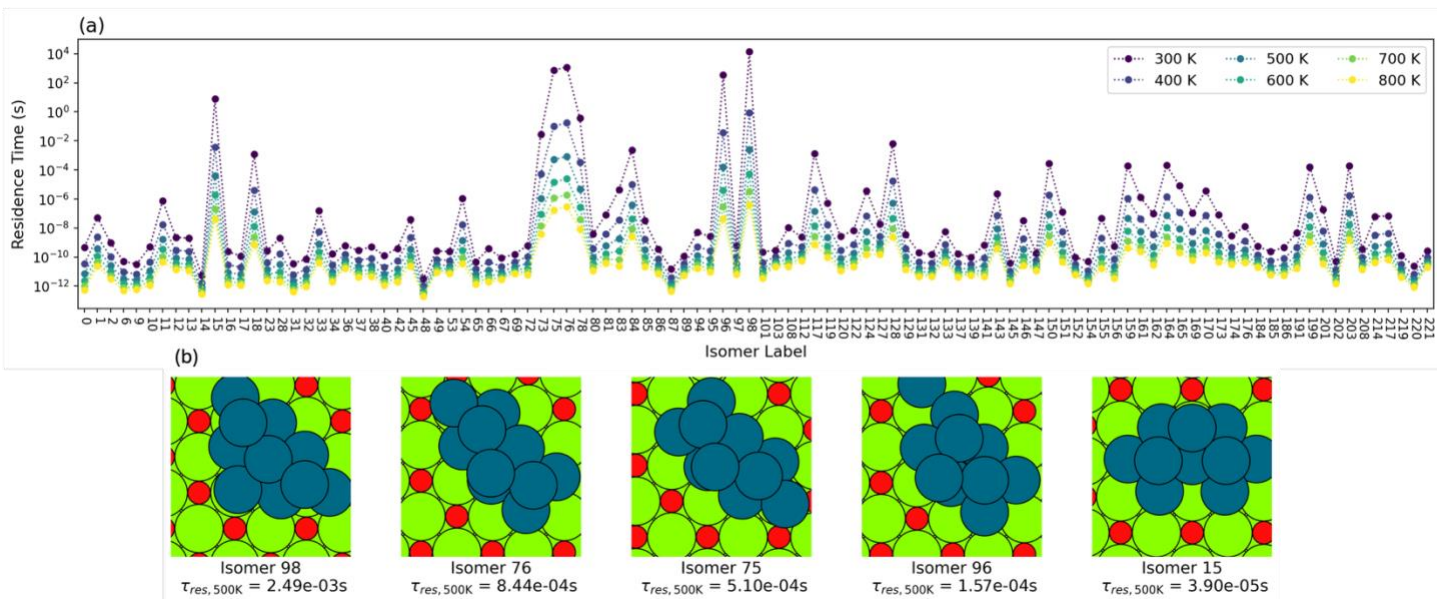


Figure S25. Pd10 residence time and top 5 dynamically stable structures

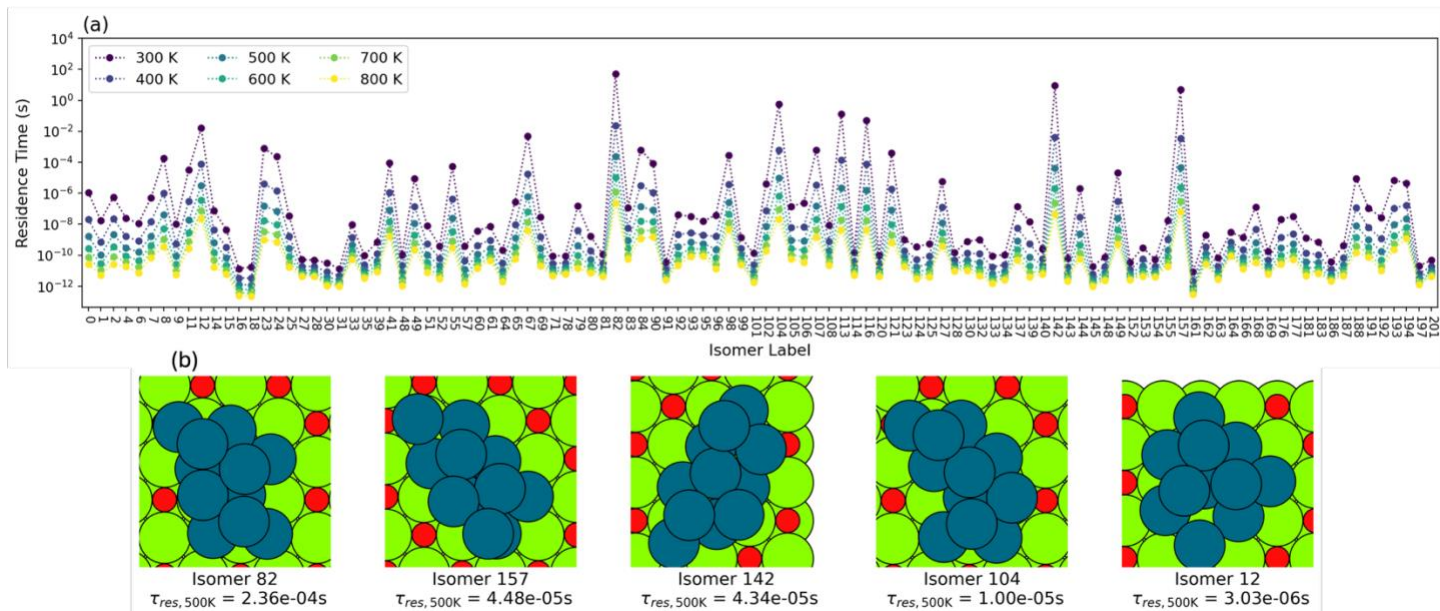


Figure S26. Pd11 residence time and top 5 dynamically stable structures

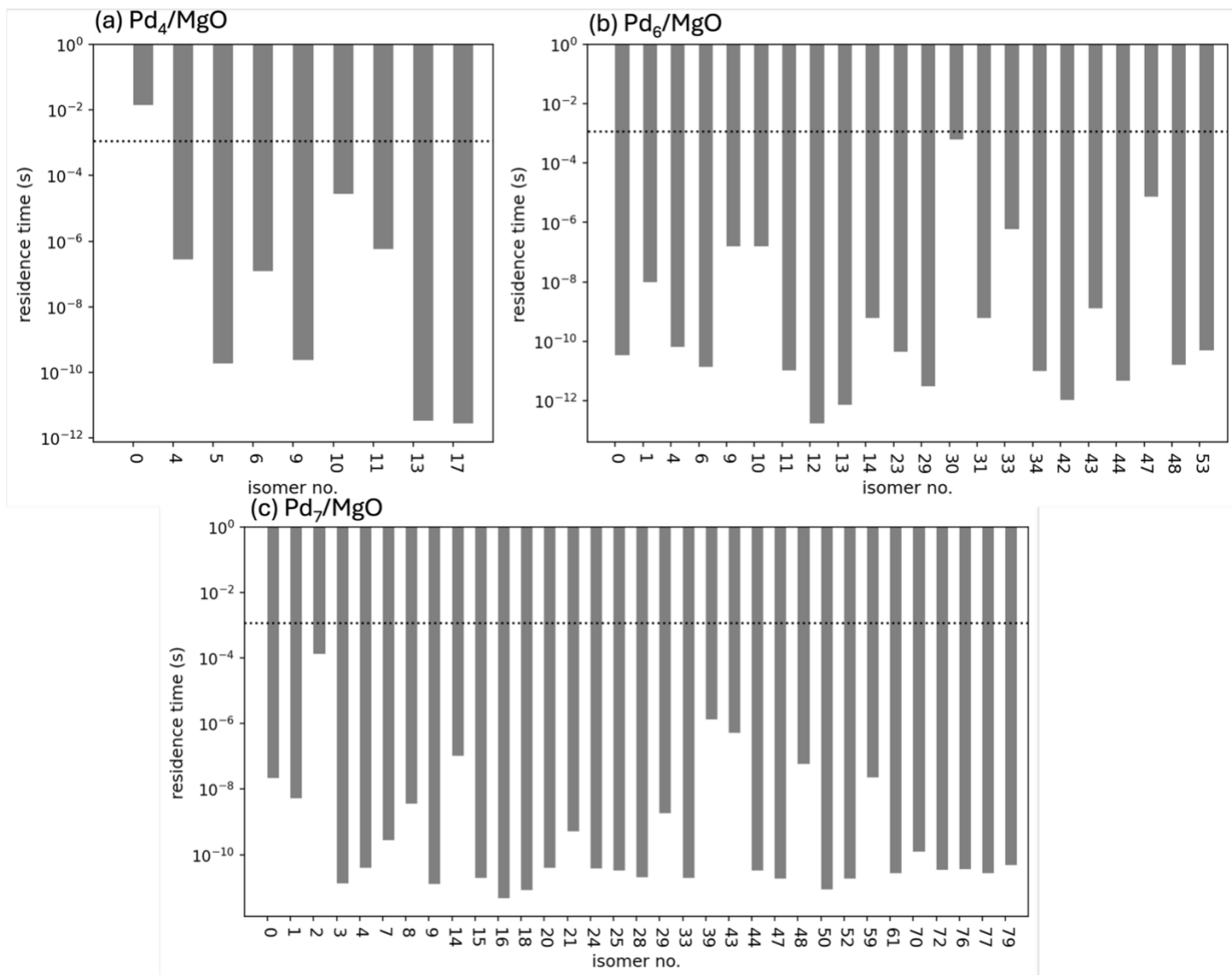


Figure S27. Histograms of per-isomer residence times at 500 K for (a) Pd₄/MgO, (b) Pd₆/MgO and (c) Pd₇/MgO, compared to the time required to overcome a 1 eV barrier (dashed line on all plots), taken as an example barrier height for the rate-determining step of a typical catalytic process. Note that virtually all isomer residence times are less than that for the 1 eV RDS.